

# A molecular dynamics study of cyclodextrin nanosponge models

Giuseppina Raffaini · Fabio Ganazzoli ·  
Andrea Mele · Franca Castiglione

Received: 19 December 2011 / Accepted: 8 February 2012 / Published online: 4 March 2012  
© Springer Science+Business Media B.V. 2012

**Abstract** Highly crosslinked polymeric networks formed by cyclodextrins (CD) have recently been shown to be highly versatile nanosponge systems, being for instance very efficient both for drug delivery and for pollutants removal. Here we report some molecular simulation results for dry and hydrated CD nanosponge models aimed to study their swelling behavior. We also report simulation results about the water mobility in these systems in terms of the calculated diffusion coefficient of “free” and of “bound” water molecules confined within the nanosponge cavities. Furthermore, we also suggest the presence of surface-constrained water molecules temporarily bound to the network surface but eventually set free in the bulk.

**Keywords** Cyclodextrin nanosponges · Molecular simulations · Molecular dynamics · Water diffusivity

## Introduction

$\beta$ -Cyclodextrin ( $\beta$ -CD) based polymers are currently receiving a great interest for the unique capability to include relatively large guest molecules by the cooperation of two or more adjacent CD moieties in a highly cross-linked polymeric network, usually denoted as a CD nanosponge. These systems have many important applications, for instance as drug delivery systems [1–4] and for pollutants removal in environmental issues [5–8]. The synthesis

and some peculiar properties of the  $\beta$ -CD nanosponges have already been reported [9]. These new nanoporous materials are prepared by reacting  $\beta$ -CD with several cross-linking agents such as pyromellitic dianhydride (PMA), carboxylic acids or activated carbonyl compounds (diphenylcarbonate DPC), as shown in Scheme 1. The choice of the cross-linking agent affects the behavior of the polymer: for example, DPC leads to quite stiff and non-swelling nanosponges, whilst PMA provides flexible and swelling nanosponges. In turn, the swelling capability of the latter can be modulated by the cyclodextrin/PMA molar ratio: the smaller the quantity of PMA, the larger the nanosponge degree of swelling, as qualitatively reported in Scheme 1.

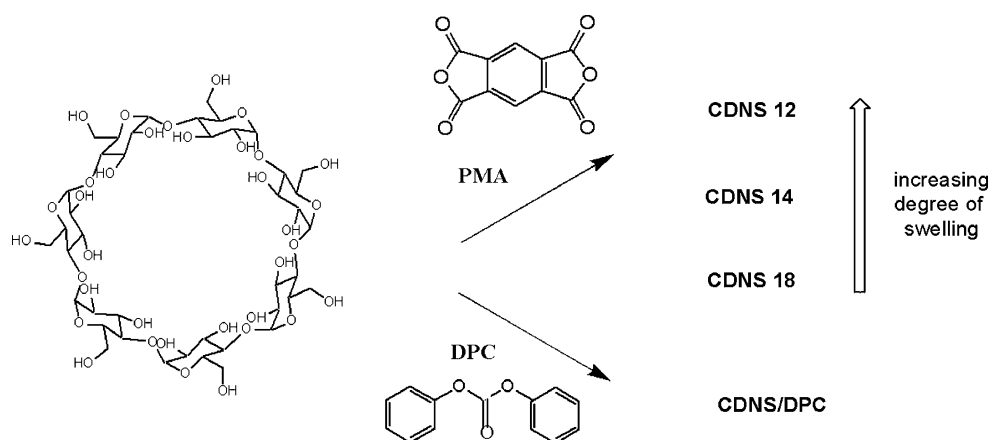
Quite surprisingly, a thorough structural and physico-chemical characterization of CDNS has been started on a systematic ground only very recently [10], despite the large repertoire of applications of CDNS summarized above that makes this class of polymers promising materials for immediate technological use. In this scenario, we here report some theoretical results based on molecular mechanics (MM) and molecular dynamics (MD) simulations on the CDNS/PMA system in a 1:1 molar ratio, simply denoted in the following as CDNS. Here we are assuming a lower content of the crosslinking agent compared to what is currently done in practice, so that, extrapolating from the observed behavior indicated in Scheme 1, we can qualitatively expect an even larger swelling of the present CDNS model compared to the experimental behavior. The present molecular dynamics simulations can provide a theoretical estimate of the CDNS swelling in water, but most importantly a quantitative value for the water diffusion coefficient that can be compared to the experimental data [10].

In fact, we recall that MM methods are based on the energy minimization with respect to all the variables

G. Raffaini · F. Ganazzoli (✉) · A. Mele · F. Castiglione  
Dip. Chimica, Materiali e Ing. Chimica ‘G. Natta’, Politecnico di  
Milano, Piazza L. da Vinci 32, 20133 Milan, Italy  
e-mail: fabio.ganazzoli@polimi.it

G. Raffaini  
e-mail: giuseppina.raffaini@polimi.it

**Scheme 1** Scheme of the synthesis of CDNS. The numbers refer to the molar ratio between reagents (e.g. CDNS 12 = polymer obtained from  $\beta$ -CD and PMA in molar ratio 1:2, respectively)



(the atomic coordinates) to optimize the system geometry in a dry or in a hydrated environment, while the MD methods follow the time evolution of the system with Newton's equations of motion at constant temperature  $T$ . Therefore the MD method permits an analysis of the kinetics of a process to equilibrium or the equilibrium fluctuations to calculate average properties at the chosen  $T$ , including also the mobility of the solvent molecules. The adopted strategy thus involves simulations both in vacuo to study the properties of a dry system, and in explicit water to study the hydration and swelling of the nanosponges, as well as the water mobility.

### Simulation methodology

The model nanosponges were generated by linking ringwise 5  $\beta$ CD (Model 1) or 8  $\beta$ CD (Model 2) and 6  $\beta$ CD with a pendant tail of 2  $\beta$ CD (Model 3) through PMA moieties (see Scheme 1). Accordingly, each CD carries two PMA linking agents bound to a primary hydroxyl at diametrically opposite sides of the macrocycle. In fact, the formation of the ester group between CD and PMA occurs mainly at the primary OH groups of the glucose units, as found experimentally through infrared and Raman spectroscopy and solid state NMR [11]. Multiple cross-links at the primary hydroxyls can also take place at larger cross-linker densities, but they are quite unlikely with the present stoichiometry.

The simulations were performed with InsightII/Discover 2000 [12], using the consistent valence force field CVFF [13]. This force field, used also in previous work [14], describes non-bonded interactions through van der Waals and Coulombic terms only, with no extra term for H-bonds. CVFF, originally designed to model proteins, was later augmented to include additional functional groups including the acetal moiety, thus accounting also for the anomeric effect in carbohydrates. Therefore, it can be satisfactorily used for these molecules [15], even though the latter effect

is not conformationally dominant in CDs because of the geometric constraint imposed by the macrocycle. Extensive tests carried out in comparison with NMR data do support the general accuracy of CVFF for oligosaccharides [14, 16]. The geometries of  $\beta$ -CD and of the model nanosponges (see later), generated with the available templates, were fully minimized in vacuo up to an energy gradient lower than  $4 \times 10^{-3} \text{ kJ mol}^{-1} \text{ \AA}^{-1}$ , and then subjected to an MD run with final energy minimizations to get the optimized geometries in vacuo of the isolated CDs. The MD simulations of the model nanosponges were performed in vacuo for 10 ns at a constant temperature ( $T = 300 \text{ K}$ ) controlled through the Berendsen thermostat, which allows for a time step of 1 fs. Integration of the dynamical equations was carried out with the Verlet algorithm, and the instantaneous coordinates were periodically saved for further analysis, while again the optimized geometries were found by final energy minimizations. In the MD runs the main changes took only place in the initial part of the simulation, and the system equilibration was monitored by the time change of the potential energy and of its components, and of relevant inter-molecular distances, in particular between the centers of mass of the individual CDs and of the whole CDNS system. A further check of the configurational changes within the whole system and of its equilibration was also carried out through the similarity maps that show similar conformations belonging to the same family of conformers through the root-mean-square distances among selected atoms (for instance of the guest and host molecules), calculated for all pairs of instantaneous conformations of the MD trajectory. For the simulations in explicit water, the geometry of the CDNS nanosponge model 1 was hydrated by adding 2,030 water molecules at the local density of  $1 \text{ g cm}^{-3}$  in a cell with edges of  $40 \text{ \AA} \times 40 \text{ \AA} \times 45 \text{ \AA}$  and periodic boundary conditions, and the MD runs were carried out for 5 ns at a constant volume (NVT ensemble), and then for further 5 ns at a constant pressure (NPT ensemble), even though the

latter run did not show any significant difference from the previous one. In the CDNS nanosponge Model 3, 4490 water molecules were added as before in a periodic cell with edges of  $50 \text{ \AA} \times 50 \text{ \AA} \times 60 \text{ \AA}$  and the MD runs were carried out for 5 ns at a constant volume only (NVT ensemble).

## Results and discussion

### Simulations in vacuo: the dry systems

The geometries of the three CDNS models were first simply optimized in vacuo (dry system), and then the resulting geometries were subjected to MD runs at 300 K with final geometry optimizations. Fig. 1 reports in the first row the geometry of the three CDNS models after the initial energy minimization, and in the second row the corresponding fully optimized geometries.

Simple visual inspection of the fully optimized systems (Fig. 1, second row) shows that in the dry state, the CDNS tend to assume a fully compact state, which is most evident for Model 3 thanks also to its dangling chain. The

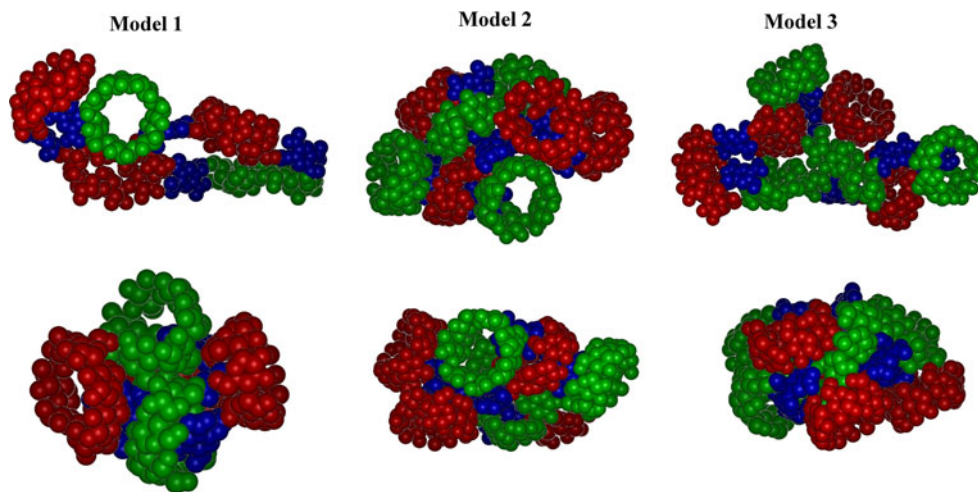
achievement of the compact state can be monitored through the time change of the distance between the c.o.m. of each CD and the c.o.m. of the whole CDNS, shown in Fig. 2. In this most compact state, the CDNS also minimizes the accessible surface area, defined as the surface area accessible to a spherical probe having a radius of  $1.4 \text{ \AA}$ , i.e., the size of a water molecule (see also later).

As a result, there is a significant clustering of the CDNS atoms near the common center of mass, as shown in Fig. 3 through the pair distribution function (PDF) of the nanosponge model atoms as a function of their distance  $r$  from the c.o.m. It should be recalled here that the PDF gives the probability density of finding a group of atoms (of the whole CDNS model, here) as a function of their distance from a given point (the c.o.m. of the whole system, here).

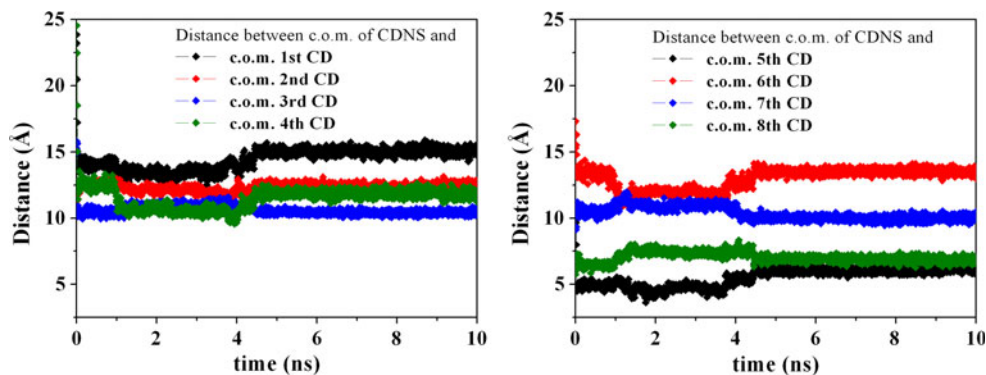
### Simulations in explicit water

For computational reasons, the simulations in explicit water (Fig. 4) were carried out only for the CDNS Models 1 and 3 starting from the most compact geometry achieved in the dry state, even though most results will only be reported for the latter model in view of the close similarity

**Fig. 1** The geometry of the three CDNS models in vacuo after the initial energy minimization (*first row*), and after full optimization after the MD runs (*second row*). For clarity, the CDs are colored in *red* and *green*, and the linking agents in *blue*. (Color figure online)



**Fig. 2** The time change of the distance between the c.o.m. of the eight CDs and the c.o.m. of the whole CDNS in the MD run in vacuo after the initial energy minimization for Model 3



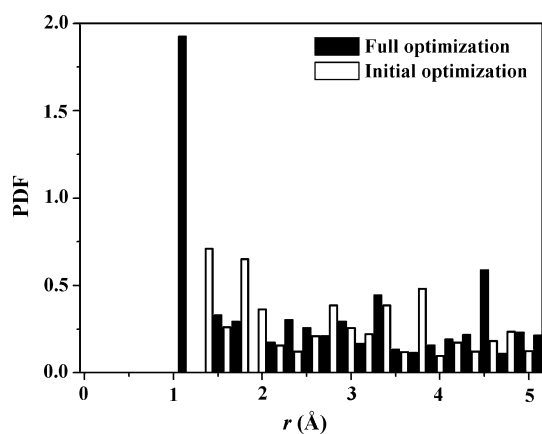


**Fig. 3** The pair distribution function (PDF) giving the (non-normalized) probability density of finding a CDNS atom as a function of its distance  $r$  from the common c.o.m

of most results. The final, optimized geometry achieved in water is shown in Fig. 4 at right. While an equilibrium state was apparently achieved, much lengthier rearrangements cannot be ruled out. In any case, the CDNS Model 3 displays a significant swelling in water, clearly limited however by the topological constraint imposed by the trial topology adopted here. Correspondingly, there is an increase of the accessible surface area. While the increase achieved after the initial minimization is quite modest (the surface area increases from 44.5 to 46.0 nm<sup>2</sup>), the swelling is more pronounced in the MD run, eventually leading to a surface area of 50.8 nm<sup>2</sup>.

The overall estimated degree of swelling for both Model 1 and Model 3 only amounts to 22%, in terms of the ratio between the swollen and the dry CDNS, i.e.  $V_{\text{swollen}}/V_{\text{dry}} = 1.22$ , as an effect of the just-mentioned topological constraint. It should be noted that experimentally the degree of swelling is often determined in terms of other quantities, such as for instance the mass ratio of the dry and

of the nanosponge fully swollen in water [10], but in any case it is much larger than what obtained here, possibly even by almost an order of magnitude. On the basis of our simulations and of the topological constraints imposed by a “perfect”, tightly interconnected network, we suggest that the observed swelling is largely boosted by topological “defects” due to missing crosslinks and dangling polymeric chains that may yield a strongly non-affine expansion at different (nano)scales. Incidentally, the proposed presence of such topological defects yielding also large cavities within the nanosponge is also consistent with the large uptake of a whole protein such as bovine serum albumin by relatively similar polyamidoamine  $\beta$ -CD nanosponges [17], even though in the latter case the linking agents are longer and more flexible than PMA or DPC.

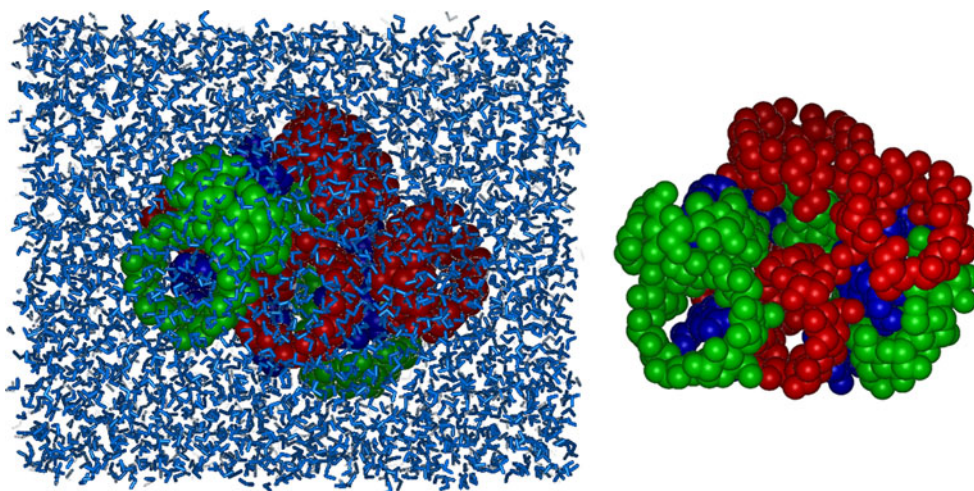
The experimental diffusivity data obtained by NMR experiments [10] indicate the presence of two types of water molecules with an unlike mobility in the swollen CDNS, involving “free” water and “bound” water. Accordingly, we calculated the diffusion coefficient of a few selected water molecules from the trajectories of the MD simulations by plotting the average mean-square displacement (or MSD) of their c.o.m as a function of time. Indeed, the MSD, defined in eq. (1) is linearly proportional to time  $t$  in the diffusive regime:

$$\text{MSD} = \langle [\mathbf{r}_i(t) - \mathbf{r}_i(0)]^2 \rangle = 6Dt \quad (1)$$

where the  $\mathbf{r}_i$ 's are the vector position of the c.o.m. of the  $i$ th molecule at the indicated time,  $D$  is the self-diffusion coefficient, and the angular brackets indicate the configurational average at equilibrium and the average over the water molecules taken into consideration. A plot of the MSD of different sets of water molecules as a function of  $t$  is shown in Fig. 5 for Model 3.

First of all, three different sets of water molecules can be clearly recognized in Fig. 5. One set corresponds to the

**Fig. 4** At left, the CDNS Model 3 after the initial optimization in explicit water. where the whole simulation box is shown. At right, the fully optimized geometry is shown after the MD run (the water molecules were canceled for clarity)



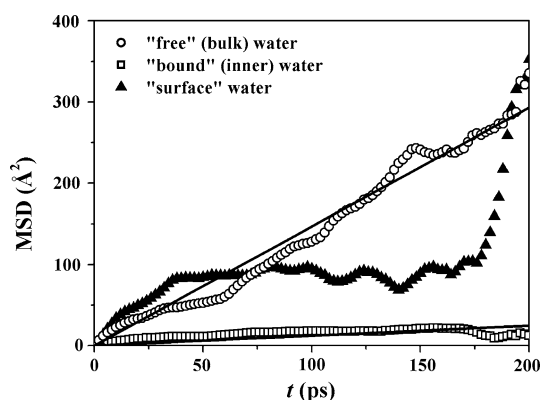


**Fig. 5** The MSD of different sets of water molecules plotted as a function of time  $t$  for Model 3. The different sets are explained in the legend (see also text)

“free” water in the bulk, showing the largest mobility at intermediate times, and the second set to the “bound” water with the lowest mobility, corresponding to the inner molecules comprised in the CDNS cavity. However, the MD simulations do also show an additional set of water molecules not detected experimentally for their relatively small number. These are the “surface” molecules (Fig. 5) characterized by a relatively well-defined plateau of MSD (in the range 30–170 ps) after the initial diffusion, corresponding to molecules temporarily “bound” for a while on the CDNS outer surface (see Fig. 4) before they can escape in the bulk.

Secondly, the slopes of the best-fit curves obtained by linear regression of the simulation data in Fig. 5 are equal to  $6D$ , thus allowing extracting the self-diffusion coefficients for the “free” and the “bound” (inner) water molecules. The resulting values are reported in Table 1 in comparison with experimental results obtained in Ref. [10] through high resolution magic angle spinning NMR (HRMAS NMR) experiments. As it can be seen, the agreement between the experimental results and the calculated values for “free” and for “bound” water is very good. Even though the excellent agreement with the reference value might possibly be fortuitous, in any case the

**Table 1** Self-diffusion coefficients ( $\text{m}^2/\text{s}$ )

System	$D$ (“free” water)	$D$ (“bound” water)
Model 3 (this work) <sup>a</sup>	$2.44 (2) \times 10^{-9}$	$2.05 (9) \times 10^{-10}$
CDNS12 (exptl) <sup>b</sup>	$1.6 \times 10^{-9}$	$1.7 \times 10^{-10}$
CDNS14 (exptl) <sup>b</sup>	$2.6 \times 10^{-9}$	$6.5 \times 10^{-10}$
Reference <sup>c</sup>	$2.406 \times 10^{-9}$	–

<sup>a</sup> The value in parentheses is the estimated error on the last significant digit

<sup>b</sup> From Ref. [10]

<sup>c</sup> At 300 K, from Ref. [18]

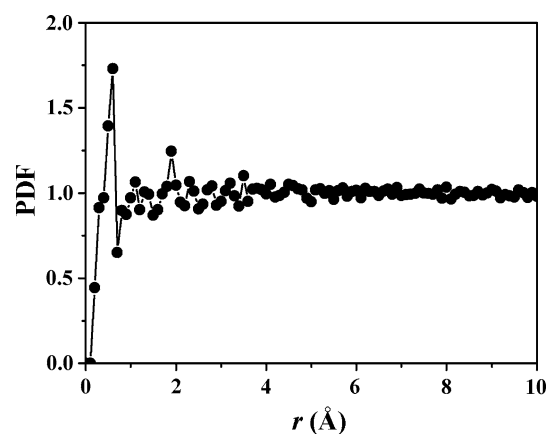


**Fig. 6** The pair distribution function PDF of the water molecules plotted as a function of the distance  $r$  from the CDNS c.o.m

calculated value have not only the correct order of magnitude, but also they nicely fall in the observed range for two different CDNS nanosponges.

We finally report in Fig. 6 the distribution of the water molecules around the c.o.m. of the CDNS (Model 3), normalized to the density of the bulk water. This plot shows in particular a sharp and quite large first peak at a distance from the c.o.m. equal to  $r = 0.6 \text{ \AA}$ , consistent with the reduced mobility of the inner “bound” water, together with the water molecules hydrogen-bonded to it that give rise to the second peak at a larger distance.

## Conclusions

Atomistic molecular dynamics simulations of a nanosponge model formed by a finite fragment of CDNS show a very compact structure in the dry state, modeled through simulations carried out in vacuo. When the explicit water solvent was introduced, the MD runs showed a significant nanosponge swelling, limited however by the topology of the model. The experimentally observed swelling was actually much larger for a real 3D network, and on the basis of the reported simulations we suggest that topological “defects” due to missing crosslinks and to dangling chains producing a non-affine expansion at different (nano)scales can be responsible of this effect. This suggestion could be tested by appropriate simulations involving appropriate CDNS models having a random and defective connectivity, and a much larger number of CDs, with obvious computational problem. We also note however that the large cavities due to the proposed topological defects are also consistent with the large uptake of albumin by a related polyamidoamine  $\beta$ -CD nanosponge [17].

The simulations in explicit water allowed to characterize the nanosponge hydration and the distribution of the water molecules inside the considered fragment and at its outer

surface. More interestingly, analysis of the mean-square displacement (MSD) of different sets of water molecules as a function of the simulation time showed the presence of “bound” inner water and of “free” bulk water in agreement with the experimentally observed behavior [10, 11]. Additionally, the simulations showed also the presence of water molecules temporarily bound to the molecular surface, that are set free to the bulk rather quickly. Moreover, the calculated self-diffusion coefficients for the “free” and the “bound” water obtained from the slope of the MSD vs. time were found to be in quantitative agreement with experimental data from HRMAS-NMR measurements [10].

## References

1. Trotta, F., Tumiatti, W., Cavalli, R., Roggero, C.M., Mognetti, B., Berta, Nicolao, G.: Cyclodextrin-based nanosponges as a vehicle for antitumoral drugs. Pat. WO 09/003656 (2009)
2. Vyas, A., Shailendra, S., Swarnlata, S.: Cyclodextrin based novel drug delivery systems. *J. Incl. Phenom. Macrocycl. Chem.* **62**, 23–42 (2008)
3. Swaminathan, S., Vavia, P.R., Trotta, F., Torne, S.: Formulation of beta-cyclodextrin based nanosponges of itraconazole. *J. Incl. Phenom. Macrocycl. Chem.* **57**, 89–94 (2007)
4. Thatiparti, T.R., Shoffstall, A.J., von Recum, H.A.: Cyclodextrin-based device coatings for affinity-based release of antibiotics. *Biomaterials* **31**, 2335–2347 (2010)
5. Mamba, B.B., Krause, R.W., Malefetse, T.J., Gericke, G., Sithole, S.P.: Cyclodextrin nanosponges in the removal of organic matter to produce water for power generation. *Water SA.* **34**, 657–660 (2008)
6. Mamba, B.B., Krause, R.W., Malefetse, T.J., Nxumalo, E.N.: Monofunctionalized cyclodextrin polymers for the removal of organic pollutants from water. *Environ. Chem. Lett.* **5**, 79–84 (2007)
7. Mhlanga, S.D., Mamba, B.B., Krause, R.W., Malefetse, T.J.: Removal of organic contaminants from water using nanosponge cyclodextrin polyurethanes. *J. Chem. Technol. Biot.* **82**, 382–388 (2007)
8. Arkas, M., Allabashi, R., Tsiourvas, D., Mattausch, E.-M., Perfler, R.: Organic/inorganic hybrid filters based on dendritic and cyclodextrin “nanosponges” for the removal of organic pollutants from water. *Environ. Sci. Technol.* **40**, 2771–2777 (2006)
9. F. Trotta, W. Tumiatti: Patent WO 03/085002 (2003)
10. Mele, A., Castiglione, F., Malpezzi, L., Ganazzoli, F., Raffaini, G., Trotta, F., Rossi, B., Fontana, A., Giunchi, G.: HR MAS NMR, powder XRD and Raman spectroscopy study of inclusion phenomena in  $\beta$ CD nanosponges. *J. Incl. Phenom. Macrocycl. Chem.* **69**, 403–409 (2011)
11. Castiglione, F., Crupi, V., Majolino, D., Mele, A., Panzeri, W., Rossi, B., Trotta, F., Venuti, V.: Vibrational dynamics and hydrogen bond properties of  $\beta$ -CD nanosponges: a FTIR-ATR, Raman and solid-state NMR spectroscopic study. *J. Incl. Phenom. Macrocycl. Chem.* In print. doi:10.1007/s10847-012-0106-z
12. Accelrys Inc. InsightII 2000; San Diego, CA. See also <http://www.accelrys.com/>
13. Dauber-Osguthorpe, P., Roberts, V.A., Osguthorpe, D.J., Wolff, J., Genest, M., Hagler, A.T.: Structure and energetics of ligand binding to proteins: Escherichia coli dihydrofolate reductase-trimethoprim, a drug-receptor system. *Proteins Struct. Funct. Genet.* **4**, 31–47 (1988)
14. Raffaini, G., Ganazzoli, F., Malpezzi, L., Fuganti, C., Fronza, G., Panzeri, W., Mele, A.: Validating a strategy for molecular dynamics simulations of cyclodextrin inclusion complexes through single-crystal X-ray and NMR experimental data: a case study. *J. Phys. Chem. B* **113**, 9110–9122 (2009)
15. von der Lieth, C.-W., Kozar, T.: Towards a better semiquantitative estimation of binding constants: molecular dynamics exploration of the conformational behavior of isolated sialyllactose and sialyllactose complexed with influenza A hemagglutinin. *J. Mol. Struct. (Theochem)* **368**, 213–222 (1996)
16. Asensio, J.L., Martin-Pastor, M., Jimenez-Barbero, J.: The use of CVFF and CFF91 force fields in conformational analysis of carbohydrate molecules. Comparison with AMBER molecular mechanics and dynamics calculations for methyl  $\alpha$ -lactoside. *Int. J. Biol. Macromol.* **17**, 137–148 (1995)
17. Swaminathan, S., Cavalli, R., Trotta, F., Ferruti, P., Ranucci, E., Gerges, I., Manfredi, A., Marinotto, D., Vavia, P.R.: In vitro release modulation and conformational stabilization of a model protein using swellable polyamidoamine nanosponges of  $\beta$ -cyclodextrin. *J. Incl. Phenom. Macrocycl. Chem.* **68**, 183–191 (2010)
18. Holz, M., Heil, S.R., Sacco, A.: Temperature-dependent self-diffusion coefficients of water and six selected molecular liquids for calibration in accurate  $^1\text{H}$  NMR PFG measurements. *Phys. Chem. Chem. Phys.* **2**, 4740–4742 (2000)